Nuclear Instruments and Methods in Physics Research 228 (1985) 267–277
North-Holland, Amsterdam

THE TASSO VERTEX DETECTOR

D.M. BINNIE, W. CAMERON, A.J. CAMPBELL, B. FOSTER, D.A. GARBUTT, C. JENKINS, W.G. JONES, J. McCARDLE, D.G. MILLER and J. THOMAS

Blackett Laboratory, Imperial College, London, SW7 2AZ, England *

H. HARTMANN

Physikalisches Institut der Universität Bonn, Germany **

R. HENSLER, M. HILDEBRANDT, D. HUBERT, A. LADAGE, B. LOHR, R.J. NOWAK [+], K. REHLICH, D. TRINES and G. WOLF

Deutsches Elektronen-Synchrotron DESY, Hamburg, Germany **

J.A. BLISSETT, B.T. PAYNE, A.G. PARHAM, D.H. SAXON and D.J. WHITE

Rutherford Appleton Laboratory, Chilton, England *

D. STROM, H. VENKATARAMANIA and SAU LAN WU

Department of Physics, University of Wisconsin, Madison, Wisconsin, USA ***

Received 26 June 1984

The design, construction and performance of a small pressurized drift chamber of low mass and high wire density is described The chamber forms part of the TASSO experiment at the PETRA e^+e^- storage ring of the DESY Laboratory. First physics results obtained with the chamber are also briefly discussed.

1. Introduction

The τ lepton and mesons and baryons containing the charm (c) and bottom (b) quarks, are all found to have lifetimes in the range 10^{-13}–10^{-12} s [1]. A device able to resolve vertices to of the order of 1 mm is in principle capable of isolating the decays of these particles produced in e^+e^- collisions. This paper describes the design, construction and performance of a pressurised drift chamber (vertex detector), installed near to the interaction point inside the TASSO detector at the e^+e^- storage ring PETRA, with the aim of tagging and measuring the decays of heavy quarks and leptons.

The vertex resolution of such a detector is a function of both its spatial measurement accuracy and the amount of multiple scattering which particles experience. Sect. 2 describes the design and fabrication of the beryllium pipe on which the detector is mounted, whose parameters were dominated by the need for minimum material before the vertex detector. Sects. 3 and 4 discuss the mechanical and cell structure of the vertex detector and the readout electronics which were designed to optimise the spatial resolution. In sect. 5 the construction of the device is described while sects. 6–8 summarise our operational experience, the determination of the space–drift time relationship and the first physics results. Sect. 9 contains our conclusions.

2. The beam pipe

The design of the tube upon which the vertex detector was mounted was dominated by four main requirements:

1. Very good vacuum characteristics, since the pipe is

* Supported by the UK Science and Engineering Research Council.
** Supported by the Deutsches Bundesministerium fur Forschung und Technologie.
*** Supported by the US Department of Energy Contract DE-AC02-76ER00881.
[+] On leave from Warsaw University, Poland.

0168-9002/85/$03.00

part of the PETRA vacuum system and must maintain a vacuum of 10^{-9} Torr.
2. A minimal number of radiation lengths of material while having at the same time sufficient strength and rigidity to allow the chamber to be pressurised to 4 bar.
3. Sufficient thickness to shield the detector from the strong electrical wake field of the passing electron and positron beams.
4. The pipe to be as opaque as possible to the flux of synchrotron radiation photons which are copiously produced in e^+e^- storage rings.

It is clear that low atomic number materials with high modulus of elasticity are preferable. Beryllium, with $Z = 4$, has an exceptionally large radiation length. While rather difficult and dangerous to machine because of its brittleness and toxicity, several companies specialise in the production of beryllium components. One of these companies [2] constructed a pipe manufactured by rolling a sheet of 1.8 mm thick beryllium and brazing along a longitudinal seam; at each end of the 40 cm length the pipe was brazed to pure aluminium extensions which in turn had been electron beam welded to aluminium/stainless steel end flanges suitable as vacuum connections into the PETRA vacuum system.

The choice of the inner radius of the pipe was a compromise between getting as close to the interaction region as possible and limiting the number of synchrotron radiation photons, both direct and reflected, striking the pipe. A study of the likely synchrotron radiation flux at beam energies of around 20 GeV indicated that an inner radius of 6.5 cm was acceptable provided further masks were installed to shadow the pipe from direct photons. Masks which limited in the vertical direction were installed at ± 3.1 m from the interaction point and elliptical masks which limited in both horizontal and vertical directions were installed at ± 4.5 m. All masks had a composite surface consisting of layers of steel, molybdenum and tungsten of thicknesses designed to minimise the number of backscattered photons.

Since the beryllium is virtually transparant to the low energy photons which are the predominant component of the reflected photon flux incident on the pipe, the inner surface of the beryllium was coated with a 15 μm layer of copper, which has very high absorption for photon energies < 50 keV. Having absorbed a photon the copper fluoresces at an energy of 8 keV. The majority of these photons are absorbed by an aluminium foil before they can reach the active volume of the chamber. If necessary xenon gas which at the pressure of the chamber has a high attenuation coefficient for 8 keV photons, can also be introduced in this region between the foil and the beryllium (see section 3). Results of tests of this procedure are described in sect. 6.

In order to monitor temperature changes, two platinum resistance thermometers were attached to the beryllium pipe at the centre and at one end. These thermometers were connected to the PETRA interlock so that dangerously large heating of the beam pipe from higher order mode losses would cause the beams to be dumped.

3. Mechanical and cell design

Fig. 1 shows the configuration of the vertex detector in the TASSO central detector.

The dimensions of the vertex detector were mainly determined by the constraints imposed by the configuration of the TASSO detector. In the previous section the constraints on the inner radius of the detector were discussed; the outer radius had to be smaller than the cylindrical proportional chamber (CPC) which is essential for triggering the experiment [3]. The active length of the vertex detector, 57.2 cm, was chosen to match the angular acceptance of the CPC and the large cylindrical drift chamber.

In order to resolve the individual particles produced in a hadron jet or a τ lepton decay while using single-hit electronics, a high granularity is necessary and correspondingly short drift distances were chosen for the drift cell. As the effect of the 5 kG magnetic field is therefore small, the ionisation electrons which are closest to the anode determine the timing precision. The two cathode wires give rise to a field pattern which "focusses" the wanted electrons towards the anode. There is a net electrostatic repulsion between the two close cathode wires but the consequent variation in their separation along the chamber is small as the chamber is relatively short.

Since the radial dimensions of the chamber were severely limited, the "lever arm" for vertex reconstruction was maximised by grouping cells into four inner layers, each with 72 anode wires, and four outer, each with 108 anode wires. No guard wires were used between successive layers because of lack of space. As shown in fig. 1c wires were arranged to form radial layers in which anode wires alternated with pairs of cathodes. Several advantages accrued from this arrangement: the electrostatic forces on the anodes were almost balanced and in any case purely radial; the alternating cell structure meant that two closely spaced tracks would still be recorded with two hits each in both the inner and outer groups; and, as will be shown later, optical alignment of the anodes with respect to the cathodes became possible. The maximum drift distance in a cell varies between 3.5 and 4.5 mm depending on the radial layer; the azimuthal wire spacing was chosen to match that of the CPC and to be compatible with the present modularity of the experimental trigger [3].

Because of the restricted space available at the end

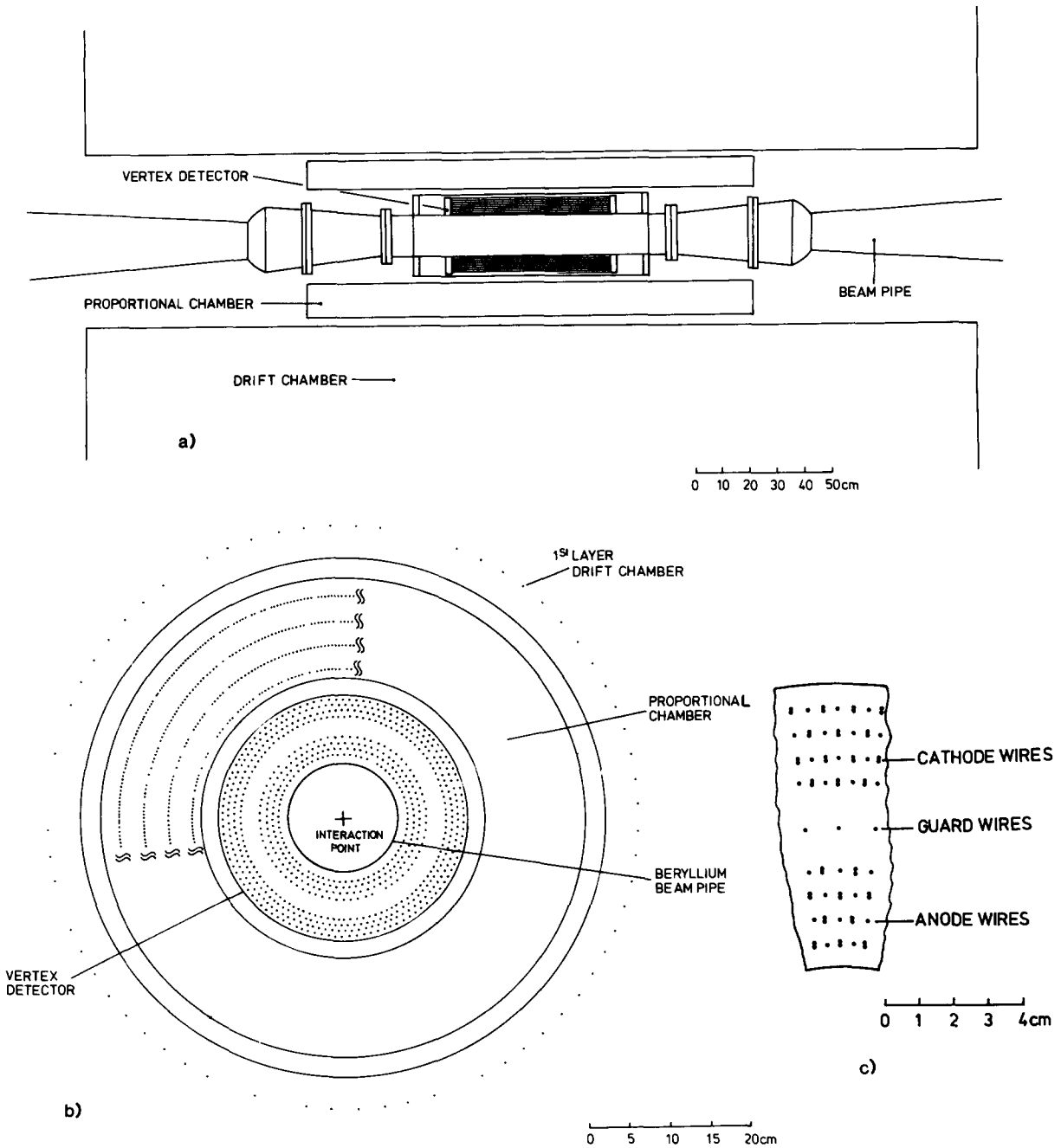

Fig. 1. (a) View of the central portion of the TASSO detector viewed perpendicular to the direction of the colliding beams. (b) The central portion of the TASSO detector viewed along the direction of the colliding beams. (c) An expanded view of part of the aluminium end flange of the vertex detector.

flange, it was decided to maintain the cathode wires at ground while raising the anodes to high voltage, thereby halving the number of electrical connections necessary and facilitating independent control of the chamber. The cathodes were therefore electrically connected to the end plates and maintained at ground.

The alignment of the anode wires to the required high precision was carried out by accurate positioning of the cathodes followed by optical alignment of the anodes with respect to the cathodes. Holes of radius 1.3 mm were drilled blind to a depth of 10 mm from the outer faces of the end plates and then radial grooves

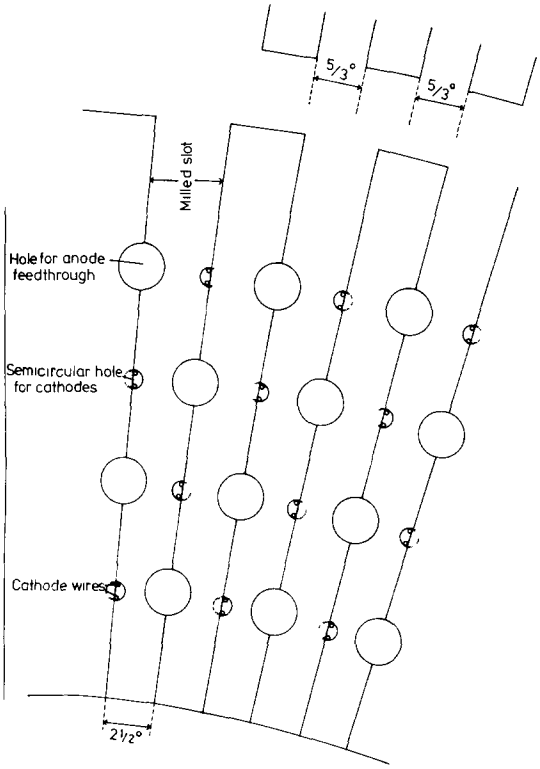

Fig. 2. A part of the aluminium end flange showing the milled slots, the holes for the anode feedthroughs and the semicircular holes for the cathode wires.

were milled from the inner sides of the plates to expose semi-circular holes as shown in fig. 2. Each pair of cathode wires was then located in the corners of this semicircle. This process defined both the wire separation and alignment. The anode wire feedthrough shown in fig. 3 was designed to allow rotation of the anode wires into line with the cathodes. It consists of an acetal body inside which the wire is held by an injection moulded acetal insert of length 3 mm and diameter 2 mm. This insert is cylindrical with a V-shaped section removed. The point of the V, which positions the sense wire, is eccentric to the centre of the insert by 200 μm. The main body of the feedthrough has two flats which allow it to be rotated using a key; thus the position of the wire held in the feedthrough can be rotated around a 200 μm radius and thereby brought into line with the previously aligned cathodes. This gave an overall r.m.s accuracy for the sense wire positioning in the crucial azimuthal direction of about 15 μm.

To complete the field configuration of the chamber, an inner equipotential formed by 50 μm thick aluminium foil at a radius of 7.6 cm was wrapped on the outside of the beryllium pipe and held at a potential of approximately 1/3 of the anode potential. Inside this equipotential a gastight compartment of 6.4 mm thick-

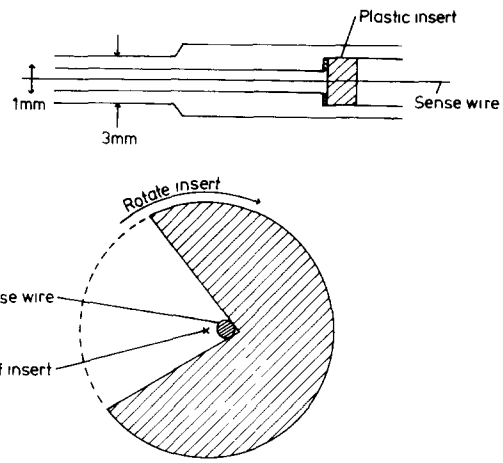

Fig. 3. *Upper* A section through the anode feedthrough. *Lower*: A cross-section through the plastic insert, illustrating how the sense wires are aligned by rotating the feedthrough.

ness was constructed which could be filled with a different gas at the same pressure as that in the vertex detector. It was intended to fill this chamber with xenon to absorb the 8 keV fluorescence photons from the copper layer on the beam pipe if these proved to cause large currents in the detector. Beyond the 8th layer of drift cells at a radius of 15.4 cm a 125 μm kapton sheet coated with 30 μm of copper was insulated from and wrapped around the end plates and connected electrically to the inner equipotential. It is a feature of the alternating cell design that the image wires reflected in these equipotential surfaces simulate approximately further cylinders of wires. A layer of 100 μm guard wires in the middle of the chamber was connected to a somewhat higher potential to collect the ionisation electrons produced in the gap between the two groups of sense wires. Finally, the chamber was enclosed in a 1.5 mm thick cylinder of aluminium and a gas seal formed betwen this and two 2 cm thick fibreglass flanges, one of which was rigidly fixed to the beam pipe, while the other was allowed to move over an O-ring to form the gas seal of the chamber. With this system the chamber could be pressurised to 4 bar.

4. Electronics design

The essential features of the electronics are shown schematically in fig. 4. The pulse initiated by the arrival of the ionisation electrons at the anode propagates down the system of wires with a characteristic impedance of 380 Ω. Wires in the first, second, fifth and sixth layers were matched at the West end only, the remainder at both ends in order to allow a charge division measurement. Between the aluminium and fibreglass

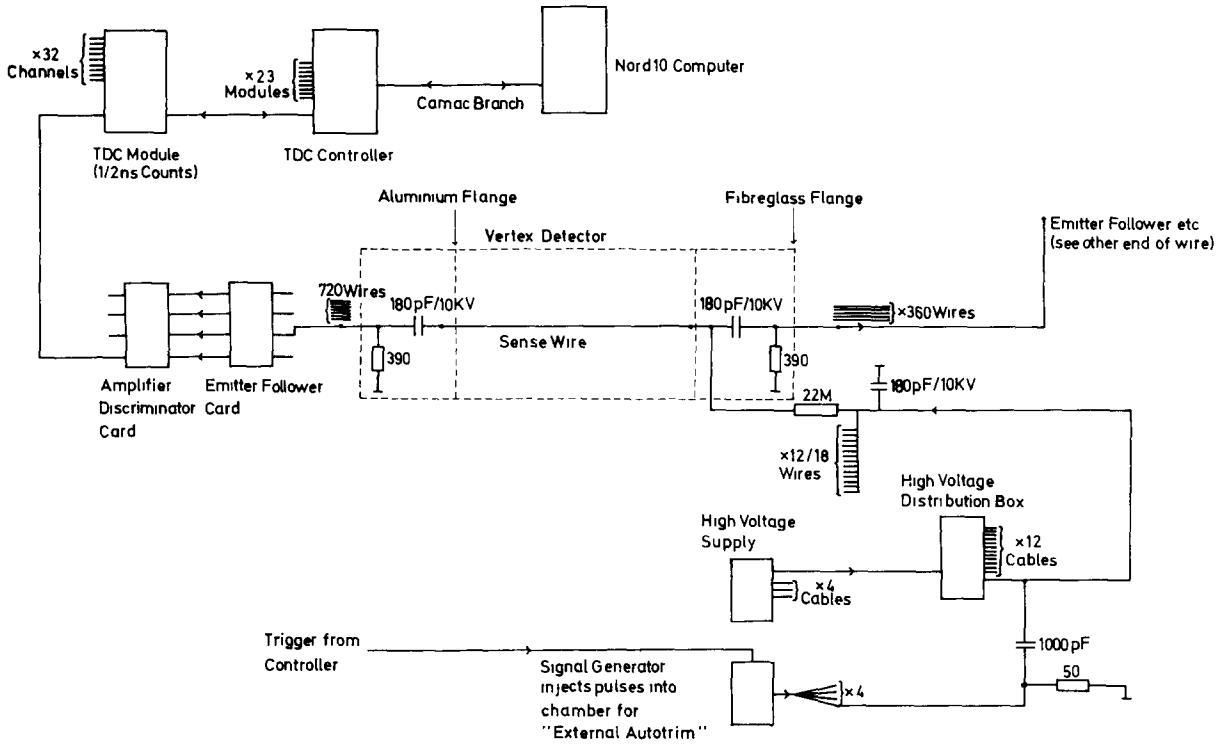

Fig. 4. A schematic layout of the vertex detector elctronic components.

flange the pulse is carried by a 180 pF coupling capacitor and adjacent "earth return" wire (one for each pair of radially adjacent cells) to a 390 Ω resistor. The layout of wires was designed to minimise coupling between adjacent cells. All wires and flanges were insulated from the beam pipe and outer pressure vessel.

High voltage was provided to the wires in 4 (radial) × 12 (azimuthal) independent groups. The inner two radial groups each supplied 12 wires, the outer two groups supplied 18 wires. This allowed not only the flexibility to switch off groups of wires in the chamber in case of very high backgrounds from PETRA but also ensured that only a small region of the chamber need be switched off in case of wire breakage. Within each group connections were made to individual wires via 22 MΩ resistors. Since there was no room for additional circuitry, calibration pulses shaped to resemble real pulses were supplied through the high voltage cables using the stray capacitance (0.3 pF) of these resistors.

Emitter-follower transistors on small printed circuit boards (pcbs) were mounted directly on the chamber. At the West end-flange each of these was used to drive 11 m of high-quality miniature coaxial cable with foam dielectric which led to a combined differential amplifier-discriminator and thereafter through 18 m of twisted pair cable to a LeCroy 4290 TDC system. Analogue signals from this end passed through 19 m of coaxial cable to two trigger processors. One of the processors was designed to detect track segments in the plane perpendicular to the beam direction which emanated from the interaction point; the other, which required outputs from both East and West ends of the vertex detector, used charge division between the two ends of each wire in the third, fourth, seventh and eight cylinders to reconstruct the z position of a track. These processors will be described in a separate publication.

The constant-fraction discriminator was designed at the Rutherford Appleton Laboratory. It is based on the Plessey SP9687 fast comparator and has particularly good slewing characteristics. The circuit diagram of the combined amplifier and discriminator is shown in fig. 5. The input circuit has to supply power to the emitter-followers on the chamber. Its input impedance is deliberately mismatched to increase the sensitivity. The differential amplifier has high common mode rejection. The emitter-follower, cable and amplifier combination has a rise time of 6 ns (10–90%).

The amplified signal passes through a 5 ns delay into the normal input and through a resistive divider into the inverting input of one of the comparators of the SP9687. The comparator senses the differential crossover point and uses it as the signal timing reference. The timing of the crossover is unaffected by signal amplitude which makes the circuit effective for reducing slew. This con-

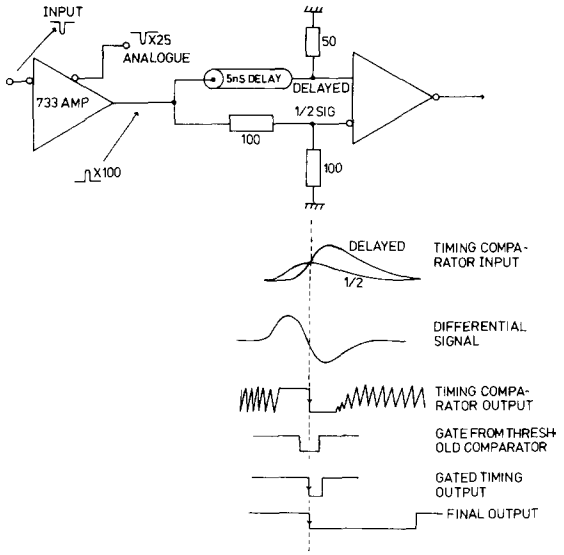

Fig. 5. A schematic layout of the amplifier/discriminator including timing diagram.

stant-faction discriminator has no threshold and works down to the system noise level, so the second comparator in the SP9687 package is used to define a threshold. Only signals greater than this threshold pass timing information on to the output pulse stretcher and differential line driver. The output pulse was made long enough (450 ns) to avoid the possibility that a second pulse could restart the time to digital convertor (TDC).

In normal operation the threshold used corresponded to a peak voltage of about 0.3 mV across the 390 Ω resistors that match the chamber wires.

The LeCroy 4290 system was used in the "common stop" mode. In this mode an input pulse to a TDC effectively initiates the counting of a train of pulses with a period of 0.5 ns. This is achieved in the usual way by a time expansion technique. A feature of the present system is that the zero time for all channels can be set with respect to externally (via a pulse generator feeding into the chamber via the high voltage supply) or internally (via a quartz clock) generated pulses. In the external mode this was used to compensate for variations in delays in the cables and circuits associated with the detector.

The possibility of electronic pickup from extraneous sources was a major concern, particularly as the cables from the two ends of the chamber of necessity followed very different paths around the TASSO magnet before coming together. A principle of the design was that magnetic flux variations in this loop should not induce signals in the amplifiers. These signals could arise either from common-mode inputs to the amplifers or from currents flowing in, for example, the outer conductors of coaxial cables. The chamber flanges and wires were electrically isolated from ground except at the point where the high voltage (h.v.) cables were connected to the chamber. Copper braiding and other shielding ran from the 0 V rail of the power supply for the amplifier cards at the West end of the chamber, along and around the signal cables to the chamber, through the outer pressure vessel of the chamber to the common earth and finally along the signal cables to the East end. Low frequency currents would therefore preferentially flow in this circuit, bypassing the amplifier inputs. The arrangement also gives some protection against high frequency noise.

With all amplifier cables connected in situ in the experiment a low level high frequency oscillation of about 120 MHz was seen on the analog outputs. The cause of this oscillation was the small amount of unavoidable cross-coupling between cards and channels tending to synchronise the freely triggering constant-fraction discriminators. This was not seen at the digital ouput since it was well below threshold, but may have been adding jitter to the system. This oscillation was almost completely eliminated by making additional connections between adjacent ground planes in the amplifier cards and by terminating the outer conductors of the input cables through 100 Ω resistors to these ground planes.

5. Construction of the chamber

The beam pipe as delivered from the manufacturer satisfied detailed requirements for dimensional accuracy and leak rate. The layer of 15 μm of copper had already been deposited on the inner surface. A 125 μm kapton sheet, formed into a cylinder and seamed on both sides with a heat-setting kapton-bonded ribbon, was used to isolate the xenon compartment from the main chamber. The ends of this sheet were then bonded to the pipe with epoxy and further strengthened by an outer bandage of kapton at each end, which also provided the gas seal. Finally the 50 μm thick aluminium foil was wrapped around the kapton to form the inner equipotential of the chamber.

The wires were strung between the 12 mm thick end flanges which were manufactured from cast aluminium sheet. The locations of the holes drilled in the end flanges were found to be on average well within the 50 μm tolerance demanded. However, the diameters of the 3 mm holes used for the anode wire feedthroughs showed significant variations and as the feedthroughs themselves, which were machined rather than injection moulded, also showed variations of the order of ± 25 μm a careful matching procedure was needed. The precision grooves used to align the cathode wires were milled under manual control to an accuracy of $\sigma = \pm 10$ μm.

The relative alignment of the two end-plates was carried out by rotating one plate with respect to the other until corresponding milled edges lay in a plane as determined by a height gauge and a surface table. The relative alignment obtained by this method was estimated to be ± 50 μm. The endplates were parallel to better than ± 0.25 mm over their diameters.

The wires used to form the cathodes of the chamber were 100 μm in diameter, made from a silver coated beryllium–copper alloy and were stretched approximately 1.2 mm by a final tension of 150 g weight. The anode wires were 20 μm in diameter and made of gold-plated tungsten–rhenium alloy with a resistance of approximately 300 Ω/m; they were soldered with a low melting-point solder (lead–tin–cadmium) to brass pins inserted in the acetal feedthroughs. They stretched by 2.0 mm under a tension of 40 g.

Several jigs were constructed in order to facilitate wire stringing in the chamber, reduce the risk of error and standardise the construction steps. A jig was positioned correctly for one hole or feedthrough by being located with respect to adjacent feedthroughs or holes and an indexing system based on the regularity of the pattern of holes ensured that the chamber was always correctly positioned. The wires were drawn through the chamber under a light tension by attaching them to needles which could be threaded through the feedthroughs or holes in either direction. Each pair of cathode wires was strung together and held by a jig in the appropriate corners of its semicircular hole ready for soldering. The correct tension was then applied using a weight over a pulley and the wires soldered in place. The appropriate tensions were calculated to allow for the increasing distortion of the end-flange as the stringing proceeded [4].

As each cylinder of wires was completed the tensions were measured by a mechanical method in which the chamber was driven tangentially by a small vibrator and the appropriate wire observed through a telescope. The resonance (at about 130 or 200 Hz for the cathode and anode wires respectively) had a full width of about 3 Hz. Most wires were within 5% of the nominal value; the 1% which were unacceptably in error were removed and replaced. A high voltage check was made by measuring the current drawn by each anode wire in air when at a potential of about 1.5 kV above the surrounding cathode wires. Any wires drawing an abnormally large current were cleaned with a fine brush dipped in ethanol; only very rarely was it necessary to replace a wire. Towards the end of construction approximately 100 anode wires or pairs of cathode wires were being strung and tested per day.

To limit the damage due to possible wire breakage a nylon thread was wound in a spiral around the central cylinder of guard wires. This was designed to prevent a broken wire in the outer four layers from reaching the inner layers and vice versa. Finally, since two anode wires became slack two days after stringing, an epoxy was applied on the inside surface of the solder pin and inside the chamber between the anode wire and the tip of the acetal feedthrough. In retrospect the latter step was possibly unwise as there was some evidence that a discharge could take place betwen the epoxy and the wire.

The optical alignment of the chamber was achieved using a telescope whose depth of focus was sufficiently small and whose lens aperture sufficiently large for any wire to be clearly seen in spite of the intervening wires. The two ends of each anode wire were adjusted independently by rotating the feedthroughs as described in sect. 3. A very small number of wires could not be exactly aligned by this method and their positions were therefore noted. The remainder were aligned to the planes defined by the cathode wires to about ± 15 μm. The alignment of all wires required 50 man hours. The feedthroughs were finally epoxied to the outer surfaces of the end flanges.

The active volume of the chamber was closed off by wrapping the outer equipotential around the two end flanges. Each free end of the copper-clad kapton sheet was pre-curved by bonding a strip of soft aluminium to it and then curving the resulting multilayer to form a good cylinder.

The electrical connection of the wires was carried out in two stages. The milled aluminium flange holding the wires was not made gas-tight, the gas seal instead being provided by the fibreglass flanges placed at a distance of 10 cm behind the aluminium flanges. At the West end 720 brass connecting pins were glued into holes drilled in the fibreglass outer flange, thus providing a tight gas seal. The connections between these pins and the outer metallic solder-spill of the feedthrough were accomplished using small pcbs containing 390 Ω terminating resistors and sliding via female connectors onto the pins in the fibreglass flange. These circuit boards were connected with flexible wires to four small, 10 kV, 180 pF capacitors covered with insulating plastic; the pcbs connected the field wires to a separate earth through another brass pin in the fibre glass flange. Care was taken to ensure that this arrangement allowed sufficient flexibility in the connectors to surmount problems caused by the extremely restricted space available between the flanges for the required components. Each pcb formed a unit connecting a group of four radial wires through the fibreglass flange; as each group was assembled good electrical connection was ensured by measuring the resistance through the sense wire to the opposite aluminium flange.

At the East end flange not only had 360 of the 720 sense wires to be connected to amplifier/discriminators to allow a charge division measurement, but also high voltage had to be fanned out to all 720 wires. This

caused even greater problems of space. The 48 separate high voltage connections were made through the fibreglass flange via brass pins to h.v. connecting sockets. Each socket was connected to 6 or 9 pcbs in the inner or outer layers respectively. The boards contained four 22 MΩ resistors "potted" and covered in insulating plastic. These resistors were connected to the solder pins of the anode wire feedthroughs via flexible wires. Each separate high voltage socket was decoupled to ground via 180 pF. In addition to these h.v. connectors the 3rd, 4th, 7th and 8th radial layers of anode wires were connected to pcbs containing two rather than four channels. Finally the chamber was enclosed in the aluminium pressure vessel.

After the assembly of the electronics at both flanges the chamber was tested using a cosmic ray trigger to ensure that all electronic channels were functioning correctly; if possible faulty channels were repaired or replaced. The whole assembly was then tested by being filled with gas at 4 bar to ensure a good gas seal and the beam pipe was connected to ion getter pumps and pumped down to a pressure of 10^{-9} Torr. When these tests had been completed the chamber was installed in the centre of the TASSO detector as shown in fig. 1.

At this stage the final electronic connections were made by plugging 180 pcbs containing emitter-follower circuits into the brass pin connectors on the West end fibreglass flange; at the East end 180 pcbs containing two emitter-followers were connected, together with 48 10 m h.v. cables linking the h.v. sockets on the flange to the high voltage supply. The h.v. supplies and monitoring circuits were constructed in a similar manner to those described in ref. [5]; experience has shown these to be very successful in protecting the main TASSO drift chamber against large current surges which can lead to wire breakage.

When the chamber had been positioned inside TASSO the final gas connections were made. The gas used was 95% argon and 5% CO_2 at a pressure of 3 bar; the choice of gas is discussed more fully in the next section. The gas supply is controlled by a thermal mass flow meter in a gas mixing unit which keeps the gas flow and the density of gas inside the chamber constant, thereby compensating for possible changes in temperature. The composition of the gas is also controlled by a mixer to within $\pm 0.3\%$.

6. Operational experience

During the short time available to test the chamber before installation in TASSO it quickly became apparent that running with a gas mixture of 50% argon and 50% ethane at 4 bar, as had originally been planned, would not be possible. During tests at anode voltages of up to 5 kV some evidence of "Whiskers", fine strands of conducting material which grow spontaneously from cathode to anode, was found. These whiskers grew with fields at the cathode surface corresponding to 50–60 kV/cm. In addition one anode wire broke close to a feedthrough and others showed signs of the epoxy close to the wire being charred and melted. Under these circumstances it was clearly desirable to run the chamber under less extreme conditions.

In order to investigate the important factors in whisker growth we constructed a small test cell consisting of a cathode wire mounted 3 mm from an aluminium plate and placed inside a glass vessel. The plate was earthed and the wire connected to a negative supply through a resistor of typically 100 MΩ. A field at the surface of the wire of 40 kV/cm was produced for each 1 kV across the gap. Argon/ethane was flushed through the chamber at atmospheric pressure and the supply voltage raised until a discharge occurred. A discharge glow could be clearly seen around the wire with a typical current of 10 μA, under which conditions the supply voltage would be −2.6 kV. After a few minutes the discharge could be seen to stabilise at one point on the wire and then move steadily across to the plate, leaving in its wake a thin black filament. During this growth the current steadily increased until the connection to the plate was completed. The filament had an estimated diameter of 20 μm and a resistance of between 100 kΩ and 1 MΩ. No qualitative change in this phenomenon was observed as the percentage of ethane in the gas was reduced. The experiment was repeated using various mixtures of argon and CO_2; in no case was any filament growth observed. Moreover, a whisker half grown in an argon/ethane mixture could be observed to burn away when this mixture was replaced by argon/CO_2. It was therefore decided to base subsequent running of the vertex detector on an argon/CO_2 mixture.

In order to minimise possible damage to the chamber from charring of the epoxy we aimed for low operating voltage. Studies using argon/CO_2 mixtures showed that it was possible to raise the pressure to 3 bar with a 95/5 mixture while running at the relatively low voltage of 2.7–2.8 kV. The drift velocity for this mixture is about 38 μm/ns compared to 50 μm/ ns obtained with 50/50 argon/ethane. Note that the absolute concentration of CO_2 in our mixture corresponds to 15% at 1 bar, thereby giving adequate quenching properties.

Running conditions for the vertex detector at PETRA energies above 20 GeV/c per beam were dominated by large background currents, with the chamber drawing a current of typically 100–250 μA depending on beam conditions. The majority of this current was concentrated in the plane of PETRA on the inside of the

* Supplied by EPCO Electronics Limited.

ring, indicating that the major contribution to the current came from off-momentum beam particles showering before the detector. Further evidence that synchrotron radiation was not a major source of current came from the xenon chamber. Much of the contribution from synchrotron radiation is intercepted by the copper coating on the beryllium and degraded to 8 keV by the fluorescence of the copper. Direct evidence for this signal was seen in the form of a monochromatic line observed during a pulse height analysis of signals from the detector during beam–beam running. This monochromatic line was observed to vanish when the xenon chamber was filled with xenon; however, the overall current in the chamber fell by only 10%.

After about 10 weeks of satisfactory operation it was found that some sectors, particularly those with large beam-induced currents, began to draw significant standing currents, even with PETRA off, and that these currents increased with time until the sectors tripped. The main features noted were that the currents drawn were much less sensitive to the applied voltage than usual; that although the chamber recovered somewhat if switched off this improvement took some hours and the behaviour quickly became bad again when switched on with circulating beams and that there were no obvious pulses on those anode wires drawing large current, suggesting that the currents were produced by a large rate of small pulses, possibly from single electrons. The origin of this effect is probably the formation of a thin layer of insulator around the cathode wires, as reported by Malter [6]. The Mark II group at PEP have reported a similar observation [7] and following a suggestion by Atac [8] had eliminated the problem by addition of ethanol vapour to the chamber gas. Because of the danger of whisker growth we wished to avoid the presence of even a few percent of such a vapour. Our present procedure is to bubble the CO_2 through ethanol at a temperature of 7.5°C and the argon through water also at 7.5°C. This procedure has given more than a year of satisfactory operation, with no sign of further problems due to this effect. Systematic studies have not been possible but there is evidence that the very small amount of alcohol introduced via the CO_2 is needed and that water alone is ineffective.

7. Determination of the vertex detector constants

In order to reconstruct the position at which a particle passed through the drift cell, it is necessary to know the relation between the measured drift time and the drift distance in the azimuthal direction. As was remarked previously, the cell design of the vertex detector is such as to make the determination of the drift velocity particularly simple. The focusing effect of the cathode wires means that the constants relating drift time to spatial position are almost independent of the entrance angle of the track.

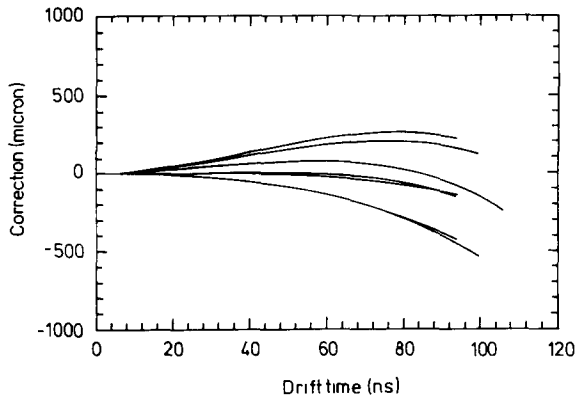

Fig. 6. The non-linear part of the space-drift time relationship for each of the eight cylinders of wires in the vertex detector.

The space–drift time relationship was determined from clean events containing two tracks originating from beam–beam interactions. An iterative procedure was used; starting with an approximation for the space–drift time relation the hits in the plane perpendicular to the beam direction in the eight vertex detector layers were reconstructed. A track was fitted from the eight points using as a constraints the absolute value of the momentum of the particle as measured in the large drift chamber which surrounds the vertex detector. For each hit on the track a residual was defined as the difference between the drift distance derived from the measured drift time and the drift distance resulting from the fitted track. For each of the eight vertex detector layers the space–drift time relation was parameterised as a third order polynomial in the drift time

$$X_i = a_i + b_i t + c_i t^2 + d_i t^3; \quad i = 1\text{–}8.$$

The 38 parameters (a–d, 3 positions and 3 angles) were

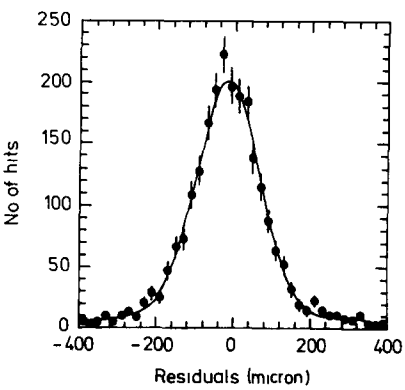

Fig. 7. Residuals for a typical cylinder of wires. The resolution fitted was 81 μm.

then fitted in order to minimise the sum of the residuals from all measured tracks. This resulted in the next approximation which allowed the hit positions to be recalculated from the drift times and the fitting of the parameters to be repeated. The whole procedure was iterated until convergence was obtained. Fig. 6 shows the non-linear part of the drift relation i.e. $x - a - bt$. As an example the distribution of residuals for layer 1 is shown in fig. 7. The r.m.s. corresponds to a spatial resolution of 81 μm. Averaged over all layers an r.m.s. resolution of 90 μm is obtained for clean two tracks events. We checked explicitly the independence of the space–drift time relation on the entrance angle of the tracks.

In order to gain the full benefit of the increased track length given by the vertex detector it is necessary to align it with the other tracking chambers very precisely. We use a method which aligns vertex detector points with tracks fitted in only the drift chamber and determined the x and y shift and the three Euler angles of the vertex detector in a simultaneous fit. The z shift is set to zero, since the z resolution is insufficient to give a good measurement of this position. The present alignment of the detector is known to 100 μm in x, y and 0.1 mrad in the Euler angles. The addition of the vertex detector points improves the momentum resolution of the TASSO detector for high momentum muon pairs to better than $\sigma/p = 0.01p$ without a beam constraint fit.

8. First physics results

Since operation of the chamber began we have collected 10.2 pb^{-1} at an average centre of mass energy of 42.48 GeV. We have used this data to obtain a sample of 37 $\tau^+\tau^-$ events where one τ decays into one charged track and the other into three charged tracks and 11 $\tau^+\tau^-$ events where both τs decay into three charged tracks. We have used these events to measure the τ lifetime, as described in more detail in ref. [9]. We determine the τ decay position and full error matrix using a fitting program, allowing the information from all three tracking chambers to be used in the fit to the vertex. The position of the production point of the τ is determined to a precision of about 150 μm in the radial coordinates on a run-by-run basis using tracks from beam–beam associated events. The size of the beam has been calculated from the PETRA optics parameters to be 500 μm horizontally and 10 μm vertically.

We constrain the production point of the τ to lie on the momentum vector of the three decay tracks and to lie within the beam envelope. The decay distance of the τ is then given by the separation of the estimated production and decay points. Fig. 8 shows the distribution of decay lengths for the 50 three-track vertices that gave acceptable fits. The distribution is clearly shifted from zero and a maximum likelihood fit to the convolution of a Gaussian measurement error with an exponential distribution gives a best estimate of the τ decay distance of $1032^{+205}_{-261} \pm 190$ μm. We have checked using Monte Carlo events and data that this result is not caused by detector or analysis bias. The measured decay distance can be converted into a τ lifetime of $(3.18^{+0.59}_{-0.75} \pm 0.56) \times 10^{-13}$ s, in good agreement with the previous measurement of ref. [10] and the expectation from lepton universality of $2.8 \pm 0.2 \times 10^{-13}$ s.

9. Conclusions

The design, construction and operation of a high precision drift chamber installed in the TASSO experiment at PETRA have been described. The chamber has been operated using a gas mixture of 95% argon, 5% CO_2 + small amounts of water vapour and alcohol at 3 bar. We have obtained the first physics result with the

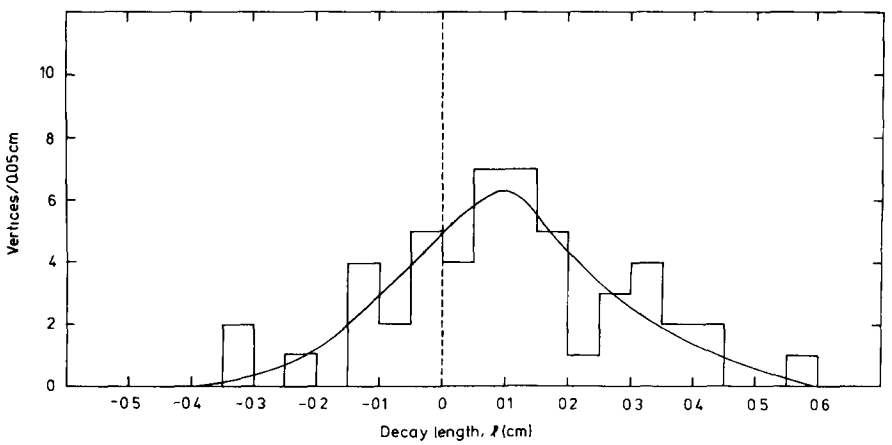

Fig. 8. The distribution of decay lengths for the decay $\tau \rightarrow 3$ charged tracks.

detector. Very satisfactory performance has been achieved in a difficult environment close to the beams at the highest energy e^+e^- interaction energies presently available.

We are very grateful to our technical staff, in particular M. Boehnert, D. Clark, F. Czempik, J. Gibb, D. Hoppe, M. Klinkmueller, W. Proelss, S. Ranga Nathan, H.H. Sabath, K. Wesphal and K.H. Wroblewski for their tremendous efforts during this project. We gratefully acknowledge the facilities and help provided to us by the Rutherford Appleton Laboratory and DESY.

References

[1] See, for instance, N.W. Reay, Proc. Int. Symp. on Lepton and photon interactions at high energies (1983) p. 244.
[2] Electrofusion Corporation, Institution Drive, Menlo Park, CA 94025, USA.
[3] S. Jaroslawski, Nucl. Instr. and Meth. 176 (1980) 263.
[4] P. Kilty, Dept. of Aeronautics, Imperial College, private communication.
[5] H. Boerner et al., Nucl. Instr. and Meth. 176 (1980) 151.
[6] L. Malter, Phys. Rev. 50 (1936) 48.
[7] J.A. Jaros, private communication.
[8] M. Atac, Fermilab preprint FN-376 2562.0000 (1982).
[9] TASSO Collaboration, M. Althoff et al., DESY 84-017 (1984) to be published in Phys. Lett.
[10] Mark II Collaboration, J.A. Jaros et al. Phys. Rev. Lett. 51 (1983) 955.